International Journal of Electrical and Computer Engineering (IJECE)
Vol. 10, No. 2, April 2020, pp. 1208~1219
ISSN: 2088-8708, DOI: 10.11591/ijece.v10i2.pp1208-1219

Torque estimator using MPPT method for wind turbines

Youssef Baala, Seddik Bri
Materials and Instrumentation (MIM), High School of Technology, Moulay Ismail University, Morocco

Article Info

Article history:

Received Sep 29, 2018
Revised Oct 15, 2019
Accepted Oct 25, 2019

Keywords:

Doubly fed induction generator (DFIG)
Kalman
MPPT
Second order sliding mode control
Wind turbine

ABSTRACT

In this work, we presents a control scheme of the interface of a grid connected Variable Speed Wind Energy Generation System based on Doubly Fed Induction Generator (DFIG). The vectorial strategy for oriented stator flux GADA has been developed To extract the maximum power MPPT from the wind turbine. It uses a second order sliding mode controller and Kalman observer, using the super twisting algorithm. The simulation describes the effectiveness of the control strategy adopted.For a step and random profiles of the wind speed, reveals better tracking and perfect convergence of electromagnetic torque and concellation of reactive power to the stator. This control limits the mechanical stress on the tansmission shaft, improves the quality of the currents generated on the grid and optimizes the efficiency of the conversion chain.

Corresponding Author:

Youssef Baala,
Materials and Instrumentation (MIN), High School of Technology,
Moulay Ismail University,
Route Agouray High School of Technology, Meknès - Morocco.
Email: ysfbaala@gmail.com

1. INTRODUCTION

When it is desired to obtain efficient transient regimes (short response time, limited overrun, etc.) and robustness with respect to external disturbances in order to control the asynchronous machine, the control scheme based on the "transient" or "Dynamic"of the machine is the vector control of the machine [1, 2]. This type of control makes it possible to have a faster response dynamics and a better accuracy of the torque control. Furthermore, PID family controllers rely on a state model with constant coefficients where system parameters are assumed to be accurately known, which is no longer the case for the asynchronous machine where some of its variables Are inaccessible to the direct measurements (rotor flux) and its parameters (in particular the time constant) are affected by the thermal effect and saturation, thus leading to limited performance.For this, the use of non-linear ordering techniques was timely and justified. Indeed, the control technique with variable structures (CSV), known for its simplicity, speed and robustness with regard to external perturbations and parametric variations, was widely adopted and showed its effectiveness in many applications. Our contribution was based on nonlinear control techniques aimed at optimizing the control of GADA [3-5]. We will start by modeling the wind turbine and its transmission chain then model the observer of the torque and the controller MPPT then a model of the machine DFIG followed by the model of the high controller sliding mode.

2. RESEARCH METHOD

2.1. Modeling the part mechanics

The maximum energy that can be collected by a wind turbine can not in any case exceed 59% of the theoretical kinetic energy of the mass of air passing through it.Currently 60 to 70% of this power can be exploited by the most sophisticated gears. This is the problem addressed by designers who aim to develop

robust and reliable MPPT algorithms for maximum power point monitoring in order to optimize energy efficiency. The wind turbine is composed of a turbine with its own parameters defining its potential to capture the energy of the moving air mass [6-8]. A judicious choice of the control strategies of the conversion chain makes it possible to obtain a system with a minimum cost and energy efficient enough, regardless of the intermittence of the wind and the variation of the load.We opted first for a model of the mechanical part (turbine and speed multiplier), and this for the 1.5 MW wind turbine, commonly used in current wind systems. Figure 1 summarizes the basic elements of the mechanical part of a wind energy conversion chain [9]. Figure 2 shows the structure of the production of energy around a DFIG.

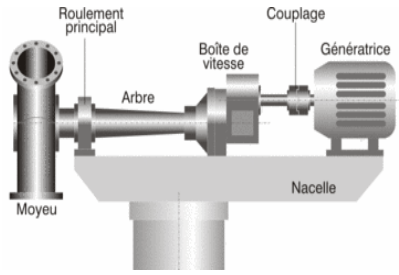

Figure 1. Basic elements of the mechanical part of a transmission chain

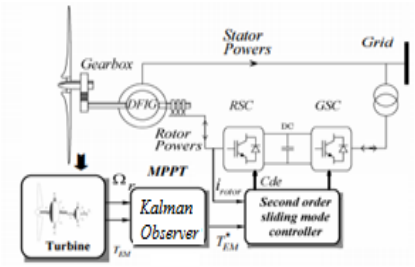

Figure 2. Control strategy

2.1.1. Modeling the wind turbine

The aerodynamic power of the wind is expressed as a function of the air density ρ, the blade radius Rpâle, the wind speed Vvent and the power coefficient Cp by relation 1 [10].

$$\text{Paero} = \frac{1}{2}.\text{Cp}(\beta,\lambda).\rho.\pi.\text{Rp}^2.\text{Vvent}^3 \quad (1)$$

The efficiency of the turbine, called the power coefficient Cp, is specific to each wing Figure 3. It depends on the angle of setting of the pales β and the specific ratio of the velocities λ. If Ωt is the rotor speed, the velocity specific ratio λ is defined as :

$$\lambda = \frac{\Omega t\,.\text{Rpale}}{\text{Vvent}} \quad (2)$$

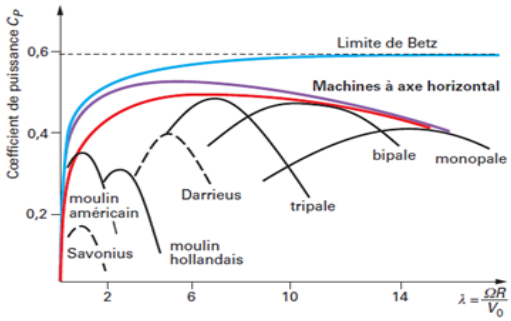

Figure 3. Limits of the power factor for different technologies

The power coefficient Cp (λ, β) for different values of the calibration angle β of a wind turbine of 1.5 MW with three pales is approximated by relation 3 [11].

$$\text{Cp}(\beta,\lambda) = \text{c1}.\left(\frac{\text{c2}}{\lambda\text{i}} - \text{c3}.\beta - \text{c4}\right)\text{e}^{-\frac{\text{c5}}{\lambda\text{i}}} + \text{c6}.\lambda \quad (3)$$

$$\frac{1}{\lambda\text{i}} = \frac{1}{\lambda - 0.08\,\beta} - \frac{0.035}{\beta^3+1} \quad (4)$$

The six coefficients c1.c6 depend on the turbine studied as show in Table 1. In the case of the E-40 turbine, proposed by the German manufacturer ENERCON, these coefficients are [12-13].

Table 1. Coefficients of the E-40 turbine

c1	c2	c3	c4	c5	c6
0 .5176	116	0.4	5	21	0.0068

Figure 4 shows the variations of the power coefficient Cp as a function of the ratio specific velocity λ, parameterized as a function of the setting angle β. These curves have a maximum for a wedge angle β = 0. In the following, the wedge angle of the pales will be fixed at a zero value (β = 0). The wind speed can then be expressed by the relation:

$$\text{Vvent} = \frac{\Omega t . \text{Rpale}}{\lambda} \tag{5}$$

For each wind speed Vvent there corresponds an optimal value of the speed of the rotor Ωopt.

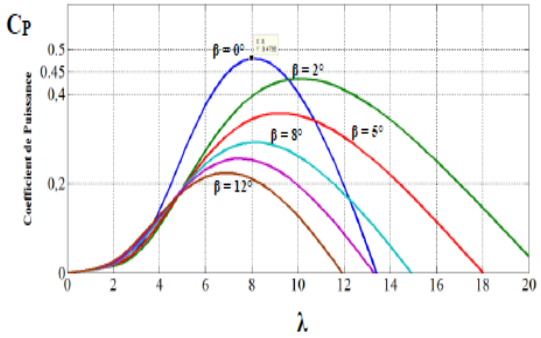

Figure 4. Variation of the Cpas a function of the reduced speed λ for different values of β

When the specific ratio of speeds λ is fixed at its optimum value. The power point optimal is characterized by: (β = 0 °; λopt = 8.1; Cpmax= 0.48). Under these conditions, the maximum aerodynamic power produced is expressed by [14-15].

$$\text{Paero} = \frac{1}{2} . \text{Cpmax} . \rho . S . \text{Vvent}^3 \tag{6}$$

It corresponds an aerodynamic torque:

$$\text{Taero} = \frac{\text{Paero}}{\Omega t} = \frac{1}{2} . \text{Cp}(\lambda, \beta) . \rho . S . \frac{\text{V}^3\text{vent}}{\Omega t} \tag{7}$$

Figure 5 shows the optimum mechanical power, recovered by the turbine, as a function of the angular speed of the rotor.

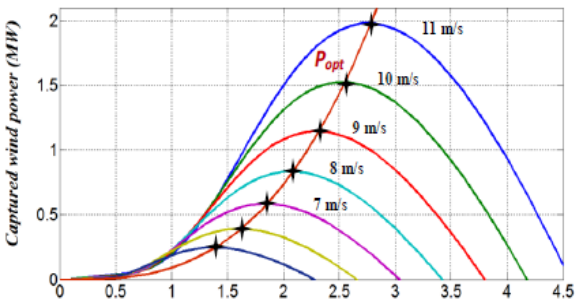

Figure 5. Variation of mechanical power as a function of turbinerotation Ωt

The optimum mechanical power Popt is given by [16]:

$$Popt = \frac{1}{2}.\rho.\pi.Rpale^5.V\frac{Cpmax}{\lambda opt^3}\Omega t^3 = Kopt.\Omega t^3 \quad (8)$$

$$Kopt = \frac{1}{2}\rho.\pi.Rpale^5.V\frac{Cpmax}{\lambda opt^3} \quad (9)$$

2.1.2. Modeling the mechanical shaft

The speed of the turbine is much less than the speed of the generator. Therefore, in one conventional wind energy conversion system, the mechanical transmission by means of a speed multiplier whose main role is to adapt the speed of rotation of the turbine to that of the generator. The multiplier thus connects the shaft of the turbine to the shaft of the generator. The two-mass model for the drive of Figure 6 is widely used [17].

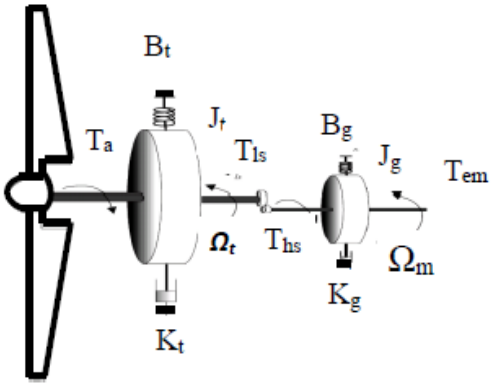

Figure 6. Mechanical coupling (turbine, multiplier, generator)

Considering the coefficients of friction (Kt, Kg) and damping (Bt, Bg), we obtain the following equations:

$$Jt.\dot{\Omega}t = Ta - Kt.\Omega t - Bt.\theta t - Tls \quad (10)$$

$$Jg.\Omega m = Ths - Kg.\dot{\Omega m} - Bg.\theta m - Tem \quad (11)$$

we obtain:

$$\frac{Jt}{Ng}\dot{\Omega m} = Ta - \frac{Kt}{Ng}\Omega m - \frac{Bt}{Ng}\theta m - \frac{Tls}{Ng}$$
$$Jg\,\dot{\Omega m} = Ths - Kg.\Omega m - Bg.\theta m - Tem \quad (12)$$

With: $$Ng = \frac{\Omega m}{\Omega t} = \frac{Tls}{Ths} \quad (13)$$

The fundamental relationship of the dynamics of rotating masses brought back to the generator shaft is written:

$$J.\dot{\Omega m} = Tm - K.\Omega m - B.\theta m - Tem \quad (14)$$

If one neglects the rigidity, the expression of the dynamics of the turbine becomes:

$$J.\dot{\Omega m} = Tm - K.\Omega m - Tem \quad (15)$$

The model of the turbine developed under matlab simulink is represented by Figure 7.

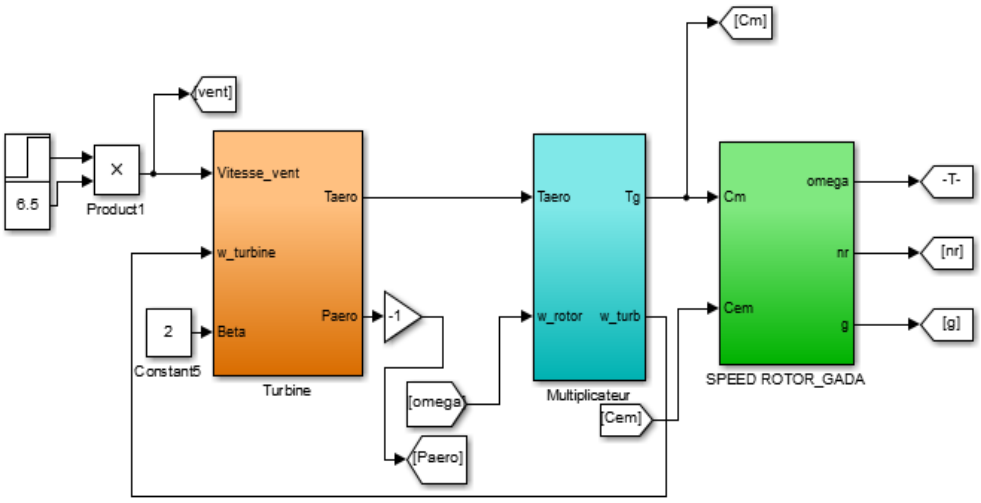

Figure 7. Wind-turbine model

2.2. Design of the MPPT control

2.2.1. Mechanical torque observer

The MPPT control ensures the convergence of mechanical torque to its optimal value in a finite time [18]. The KALMAN observer is then used to estimate the value of the mechanical torque with state variables x1 and x2 representing the speed of the rotor Ωr and the image of the mechanical torque Tm.

$$x1 = \Omega r \; ; x2 = \frac{Tm}{J} \tag{16}$$

The expression of the dynamic of the turbine become:

$$\dot{x1} = x2 - \frac{Tem}{J} - \frac{f.x1}{J} \; ; \dot{x2} = f(t) \tag{17}$$

We can rewrite this subsystem in matrix form:

$$\dot{X} = A.X + B.Tem \; ; Y = C.X \tag{18}$$

With: $X=(x1 \;\; x2)^T$ $A=\begin{pmatrix} \frac{-f}{J} & 1 \\ 0 & 0 \end{pmatrix}$ $B=\begin{pmatrix} \frac{-1}{J} \\ 0 \end{pmatrix}$ and $C=(1 \;\; 0)$ (19)

The observer is based on the following state transformation:

$$\begin{cases} \dot{\hat{X}} = A.\hat{X} + B.\dot{Tem} + H.\left(y - C.\hat{X}\right) \\ H = (h1 \;\; h2)^T \\ \hat{y} = C.\hat{X} \end{cases} \tag{20}$$

The resulting estimation error is then written:

$$\tilde{X} = X - \hat{X} \tag{21}$$

The dynamic of the errors is governed by the following:

$$\dot{\tilde{X}} = \dot{X} - \dot{\hat{X}} = (A - H.C).\tilde{X} \tag{22}$$

AO = A - H . C, is chosen so that it is a Hurwitz matrix by appropriate choice of vector H, $\dot{\tilde{X}} = \dot{X} - \dot{\hat{X}}$ is sure to converge exponentially to 0. The dynamics of the estimated states is expressed by [19]:

$$\dot{\widetilde{x1}} = \widetilde{x2} - \frac{Tem}{J} - \frac{f.\widetilde{x1}}{J} + h1.\widetilde{x1} \; ; \dot{\widetilde{x2}} = h2.x1 \tag{23}$$

2.2.2. MPPT controller design

The control must force the value of the mechanical torque Tm to follow the optimum value Top in order that the tracking error is canceled [20].

$$eT = Topt - \widehat{Tm}\ ; \widehat{Tm} = J.\widehat{x2} \tag{24}$$

The equation of the dynamics of the turbine makes it possible to write the equations of the dynamics of the tracking error as follows:

$$\dot{eT} = \dot{Topt} - \dot{\widehat{Tm}} \qquad \dot{eT} = 2.kopt.\frac{\Omega r}{J}.(\widehat{Tm} - Tem - f.\Omega r) - \dot{\widehat{Tm}} \tag{25}$$

In order to stabilize the system, taking as the Lyapunov function candidate:

$$V = \frac{1}{2}.eT^2 + \frac{1}{2}.\tilde{X}^T P \tilde{X} \tag{26}$$

Where P is a positive matrix such as:

$$A0^T P + P\,A0 = -I2 \tag{27}$$

The dynamic of the Lyapunov function is:

$$\dot{V} = \dot{eT}\,eT - \frac{1}{2}\tilde{X}^T\tilde{X} \tag{28}$$

The actual reference of the Tem^* electromagnetic torque is made with the choice:

$$eT = -d.eT \tag{29}$$

If d is a positive synthetic constant, the control law is chosen as follows:

$$V = -d.eT^2 - \frac{1}{2}\tilde{X}^T\tilde{X} < 0 \tag{30}$$

We deduce the control law backstepping of controller:

$$Tem^* = \widehat{Tm} - f.\Omega r + \frac{J}{2.Kopt.\Omega r}\,(d.eT - \dot{\widehat{Tm}}) \tag{31}$$

The model of the Kalman observer designed under matlab simulink is represented by Figure 8.

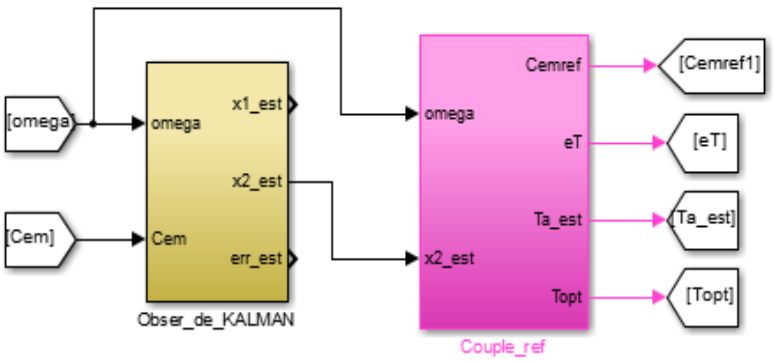

Figure 8. Kalman observer

2.3. Modeling of the DFIG

The electrical equations of the DFIG can be written as follows [21]:

$$\begin{cases} vsd = Rs.isd + \frac{d\Phi sd}{dt} - \omega s.\Phi sq \ \text{ and } \ vsq = Rs.isq + \frac{d\Phi sq}{dt} + \omega s.\Phi sd \\ vrd = Rr.ird + \frac{d\Phi rd}{dt} - \omega r.\Phi rq \ \text{ and } vrq = Rr.irq + \frac{d\Phi rq}{dt} + \omega r.\Phi rd \end{cases} \tag{32}$$

$$\begin{cases} \Phi sd = Ls.isd + Lm.ird \quad and \quad \Phi sq = Ls.isq + Lm.irq \\ \Phi rd = Lr.ird + Lm.isd \quad and \quad \Phi rq = Lr.irq + Lm.isq \end{cases} \tag{33}$$

Ls,Lr and Lm :stator,rotor and magnetizing inductances and σ : leakage coefficient $\sigma = 1 - \frac{Lm^2}{Ls.Lr}$
ωr=ωs-p.Ωr :pulsation of rotor currents and p: number of pole pairs of DFIG.
The stator, rotor active and reactive powers are defined by:

$$\begin{cases} Ps = vsd.isd + vsq.isq \quad Qs = vsq.isd - vsd.isq \\ Pr = vrd.ird + vrq.irq \quad Qr = vrq.ird - vrd.irq \end{cases} \tag{34}$$

The electromagnetic torque is defined as:

$$Tem = p.Lm.(ird.isq - irq.isd) \tag{35}$$

By setting the quadratic component of the stator flux to the null value and assuming that the resistance of the stator winding Rs is neglected, the voltage equations and the flux equations of the stator windings can be simplified in steady state as: $\Phi sd = \Phi s$; $\Phi sq = 0$ and $vsd = 0$ ($Rs = 0$)

$$\begin{cases} isq = \frac{-lm}{ls}.irq \quad isd = (\Phi s - lm.ird).\frac{1}{ls} \\ \Phi rq = lr.\sigma.irq \quad \Phi rd = lr.\sigma.ird + \frac{lm}{ls}.\Phi s \\ vrd = Rr.ird + lr.\sigma.\frac{dird}{dt} - lr.\omega r.\sigma.irq \\ vrq = Rr.irq + lr.\sigma.\frac{dirq}{dt} - lr.\omega r.\sigma.ird + \Phi s.\frac{lm.\omega r}{ls} \end{cases} \tag{36}$$

The stator active and reactive powers are obtained:

$$Ps = -Us.\frac{lm}{ls}.irq \quad Where \quad Us=\sqrt{3}.Vs \tag{37}$$

$$Qs = Us.(\frac{\Phi s}{ls} - \frac{lm.ird}{ls}) \tag{38}$$

$$Tem = -p.\frac{lm}{ls}.\Phi s.irq \tag{39}$$

$$Pr = g.Pem = g.Cem.\Omega r \tag{40}$$

The model of DFIG designed under matlab simulink is represented by Figure 9 (refer appendix).

2.4. High order sliding mode controller

This section shows the design of the proposed high-order sliding mode controller based on the super-twisting algorithm [22]. The second order sliding mode algorithm synthesizes ad is continuous control, which makes the surface and its derivative null with continuous control, therefore reducing chattering and avoiding strong mechanical efforts while preserving classical sliding mode advantages. To ensure the DFIG electromagnetic torque and reactive stator power convergence, the d-q rotor currents references are defined:

$$irq^* = -Tem^*.\frac{ls}{p.M.\Phi sd} \quad And \quad ird^* = \frac{\Phi sd}{M} - Q^*.\frac{ls}{M.Us} \tag{41}$$

Two sliding functions Sq and Sd are defined by:

$$\dot{Sq} = \frac{1}{lr.\sigma}\left(vrq - Rr.irq - Lr.\omega r.\sigma.ird - \frac{M.\omega r}{ls}.\Phi sd\right) - \frac{dirq^*}{dt} \tag{42a}$$

$$\dot{Sd} = \frac{1}{lr.\sigma}(vrd - Rr.ird + Lr.\omega r.\sigma.irq) - \frac{dird^*}{dt} \tag{42b}$$

By introducing two terms G1 and G2, such as [23]:

$$G1 = \frac{1}{lr.\sigma}\left(-Rr.irq - Lr.\omega r.\sigma.ird - \frac{M.\omega r}{ls}.\Phi sd\right) - \frac{dirq^*}{dt}$$
$$\text{And} \quad G2 = \frac{1}{lr.\sigma}(-Rr.ird + Lr.\omega r.\sigma.irq) - \frac{dird^*}{dt} \tag{43}$$

The second derivatives of the slip functions are then given by:

$$\ddot{Sq} = \frac{1}{lr.\sigma}.\dot{vrq} + \dot{G1} \quad \text{and} \quad \ddot{Sd} = \frac{1}{lr.\sigma}.\dot{vrd} + \dot{G2} \tag{44}$$

The second order sliding mode controller is based on the super twisting algorithm (ST) which was introduced by Levant as follows [24]:

$$vrq = u\&1 + u2 \quad \text{and} \quad vrd = w1 + w2 \tag{45}$$

The parameters α and θ are chosen to ensure convergence in finite time [24]-[25]:

$$\left\{\alpha i > \frac{\mu i}{lr.\sigma} \quad \theta i \geq \frac{4.\mu i.(\alpha i+\mu i)}{lr^2.\sigma^2.(\alpha i-\mu i)} \quad |\dot{G\imath}| < \mu i \;\; i = 1,2\right. \tag{46}$$

The terms of the equivalent control laws are defined by canceling the terms of the dynamics of the slip functions $\dot{Sq}$ and $\dot{Sd}$:

$$Vrdeq = Rr.ird - lr.\omega r.\sigma.irq + lr.\sigma.\frac{dird^*}{dt}$$
$$\text{and} \quad Vrqeq = Rr.irq + lr.\omega r.\sigma.ird + \Phi sd.\frac{M.\omega r}{ls} + lr.\sigma.\frac{dirq^*}{dt} \tag{47}$$

The second ordre sliding mode model designed under matlab simulink is represented by Figure 10 (refer appendix).

3. RESULTS AND ANALYSIS

The performances of the controller have been validated by means of simulation in MATLAB/ Simulink environment. The table summarizes the parameters of the controlled system Table 2. For this simulation, one of tow profiles of the wind speed is applied to the input of the turbine: step or random as shown in Figure 11. The Figure 12 shows the stator voltage is sinusoidal with maximum value 980V which corresponds to the output voltage of efficient 690V. The Figure 13 shows the current flow rate of the GADA on the three-phase to the grid. For an step turbine speed profile, the maximum current passes from 200A for a wind speed of 7 m/s to 800A for a wind speed of 14 m/s. other is done at the moment 25s is done quickly and lasts 0.01s.For an random turbine speed profile, the maximum current stator output is constant worth 800A. The Figure 14 shows the speed of the GADA. For a step turbine speed profile, the speed of the GADA goes from 700 rpm and slightly exceeds 1500rpm at the moment 25s following the wind scale. This variation corresponds to the range of speeds allowed by the GADA. For a random turbine speed profile, the speed of the rotor follows the variation of the speed of the tubine between 1000 rpm and 1600 rpm.

Table 2. System parameters

Turbine					KALMAN			Back stepping	Second order Sliding Mode	
Power (MW)	Number of blades	P	Blade longer	Multiple rapport	h1	h2		D	α1	α2
1.5	3	1.225 Kg/m3	32.25m	60	2500	25000		10^{-4}	350	0.75
			GADA					Grid	Second order Sliding Mode	
Pn	Rs	Rr	Ls	Lr	M	J	F	V	θ1	θ2
1.5Mw	12mΩ	21mΩ	13.7mH	13.6mH	13.5 mH	0.175 Kg.m2	0.0024 N/rad/s2	690-50Hz	0.5	0.06

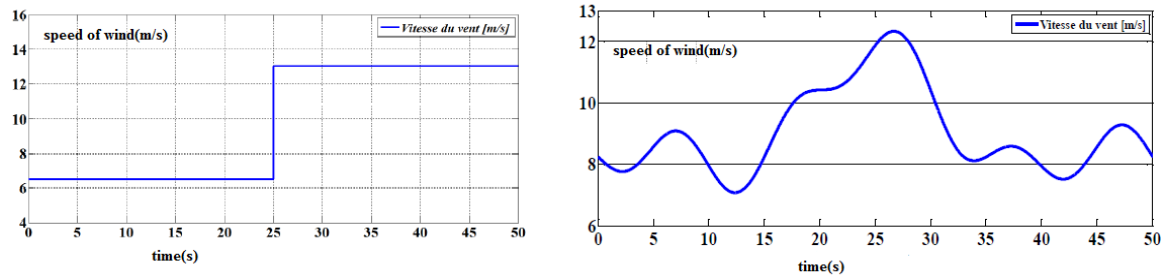

Figure 11. Variation of wind speed

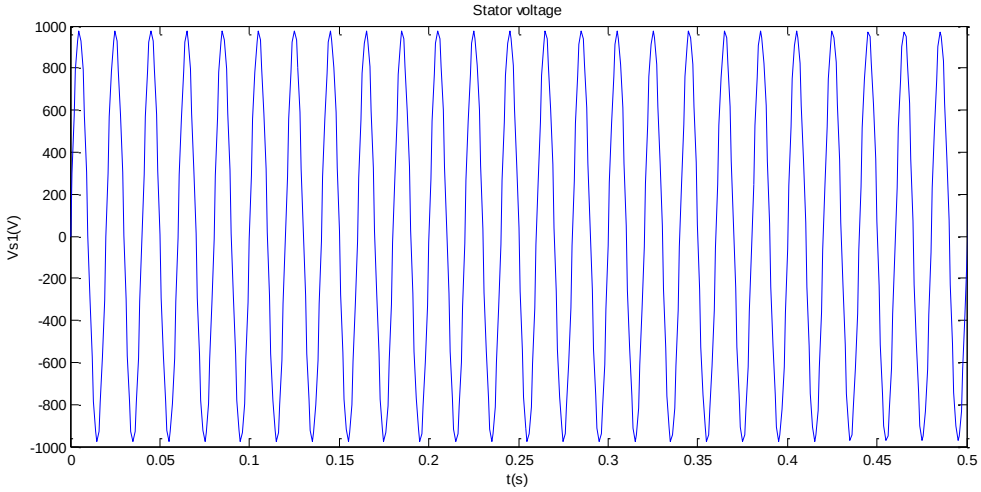

Figure 12. Stator voltage

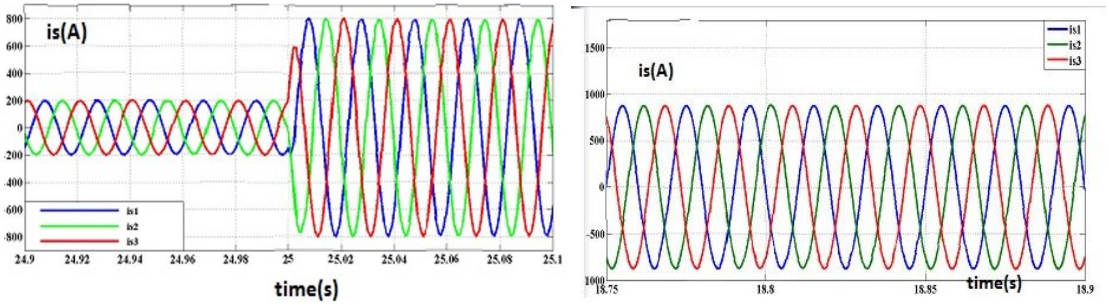

Figure 13. Stator current

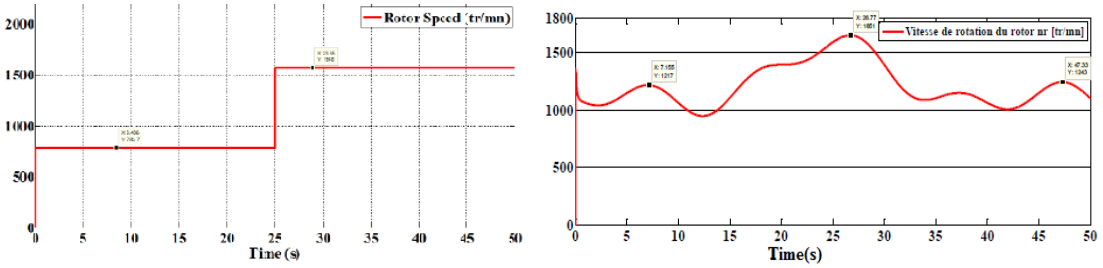

Figure 14. Rotor speed

In Figure 15 we show a perfect continuation of the electromagnetic torque at its reference delivered by the observer block of Kalman for step speed profile. We note the convergence of the electromagnetic torque Tem to wards the optional reference torque Topt. Figure 16 shows the variation of stator active power P and stator reactive power Q to the grid. Note the variation of the power Ps produced by the DFIG to the network according to the maximum point of the wind while garanteissant a unit cosφ by asservissement which guarantees the cancellation of the reactive power. We obtain a sinusoidal three-phase current output with minimal distortion.The stator reactive power Q is kept zero to guarantee a unit power factor cosφ = 1. The spectral representation of the stator current shows that this command does not introduce harmonic pollution to the grid with a harmonic distortion rate of 0.06%.

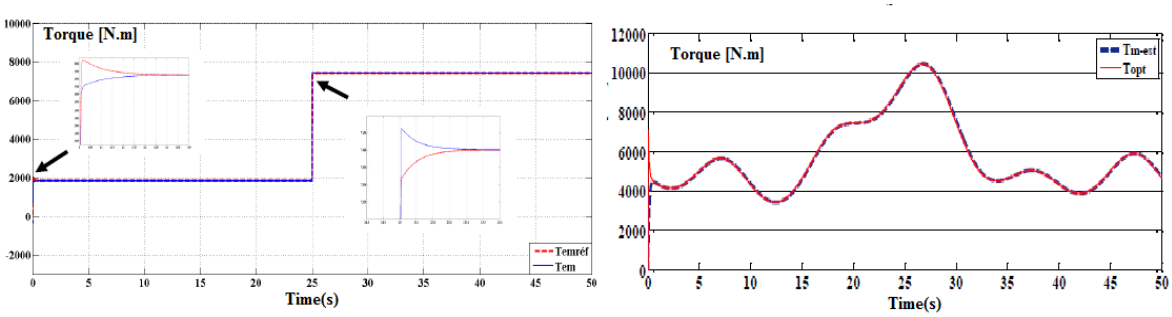

Figure 15. Electromagnetic torque

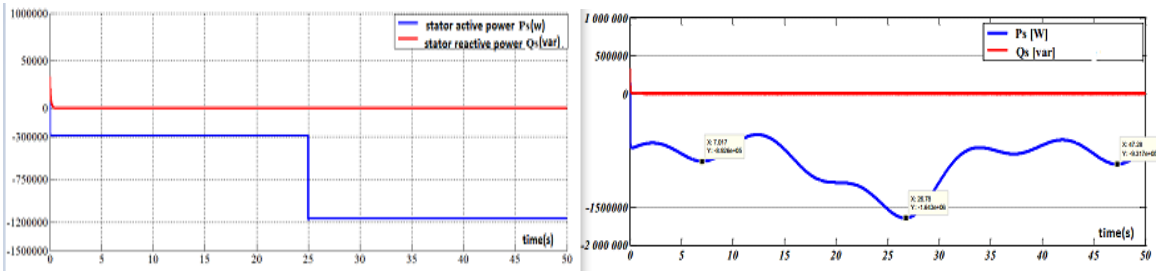

Figure 16. Stator active and reactive powers

4. CONCLUSION

To develop a command for the wind turbine generators it's necessary to use a linearization approach. However, due to conditions of stochastic operation, and inevitable uncertainties inherent in the system, such control strategies are pay at the price of a system with poor performance and decreased reliability. Hence, the use of a strategy of non-linear and robust control for taking into accounts these problems. The strategy developed and presented in this article; to know first to define the reference torque by a kalman observer combined with a command by sliding mode then in a second time to order the dual mode asynchronous generator by one mode sliding order 2, meets the assigned objectives. Indeed, she is robust thereby increasing reliability, it improves the energy efficiency, and with the little chatter she generates, it limits the mechanical stress on the tree of transmission.

REFERENCES

[1] A. Benheniche, *et al*., "A High Gain Observer Based Sensorless Nonlinear Control of Induction Machine," *International Journal of Power Electronics and Drive System (IJPEDS)*, vol. 5, no. 3, pp. 305-314, 2015.

[2] Susperregui A., Jugo J., Lizarraga I., *et al*., "Automated control of doubly fed induction generator integrating sensorless parameter estimation and grid synchronisation," *IET Renew. Pow. Gener.*, vol. 8, no. 1, pp. 76–89, 2014.

[3] M. Farshadnia, *et al*., "Current-based direct power control of a DFIG under unbalanced grid voltage," *Electrical Power and Energy Systems*, vol. 62, pp. 571–582, 2014.

[4] V. Paul-Etienne, "Order Non-Linear of Asynchronous Machine Dual Power," PhD in Electrical Engineering, National Polytechnic Institute of Toulouse, France, 2004.

[5] Boukhezzar B. *et al*., "Multivariable control strategy for variable speed variable pitch wind turbine," *Renewable Energy*, vol. 32, pp. 1273-1287, 2007.
[6] Mustapha Elyaqouti, Safa Hakim, Sadik Farhat, Lahoussine Bouhouch, and Ahmed Ihlal, "Implementation in Arduino of MPPT Using Variable Step Size P&O Algorithm in PV Installations," *International Journal of Power Electronics and Drive System (IJPEDS)*, vol. 8, no. 1, pp. 443, Mar. 2017.
[7] Youssef Majdoub, Ahmed Abbou, Mohamed Akherraz, Rachid El Akhrif, "Design of an Improved MPPT Control of DFIG Wind Turbine under Unbalanced Grid Voltage using a Flux Sliding Mode Observer," *International Journal of Power Electronics and Drive System (IJPEDS)*, vol. 8, no. 4, pp. 1723-1731, Dec. 2017.
[8] H. Becheri , I. K. Bousarhanne , A. Harrouz , H. Glaoui , T. Belbekri, "Maximum Power Point Tracking of Wind Turbine Conversion Chain Variable Speed Based on DFIG," *International Journal of Power Electronics and Drive System (IJPEDS)*, vol. 9, no. 2, pp. 527-535, Jun. 2018.
[9] N. Manonmani and P. Kausalyadevi, "A Review of Maximum Power Extraction Techniques For Wind Energy Conversion Systems," *International Journal of Innovative Science, Engineering & Technology*, vol. 1, no. 6, pp. 597-604, Aug. 2014.
[10] Dwiana Hendrawati1, Adi Soeprijanto, Mochamad Ashari, "High Performance Maximum Power Point Tracking on Wind Energy Conversion System," *International Journal of Power Electronics and Drive System (IJPEDS)*, vol. 8, no. 3, pp. 1359-1367, Sep. 2017.
[11] Valenciaga F., "Second order sliding power control for a variable speed constant frequency energy conversion system," *Energy Convers. Manage.*, vol. 51, no. 12, pp. 3000–3008, 2010.
[12] Beltran B. *et al*., "Sliding mode power control of variable speed wind energy conversion systems," *IEEE Trans. Energy Conversion*, vol. 23, no. 2, pp. 551-558, Jun. 2008.
[13] Weng, Y.T., Hsu, Y.Y., "Sliding mode regulator for maximum power tracking and copper loss minimisation of a doubly fed induction generator," *IET Renew. Power Gener.*, vol. 9, no. 4, pp. 297–305, 2015.
[14] Lingling Fan, Zhixin Miao, Xin Wang "Sensorless Maximum Power Point Tracking in Multi-Type Wind Energy Conversion Systems," *Joint 48th IEEE Conference on Decision and Control and 28th Chinese Control Conference Shanghai*, P.R. China, Dec. 2009.
[15] Khalili H.K., "High-gain observers in nonlinear feedback control," in *Proceedings of the ICCAS'08*, Seoul (Korea), Oct. 2008.
[16] Beltran B, Benbouzid MEH, Tarek Ahmed-Ali, Herve Mangel, "DFIG-based wind turbine Robust Control Using High-Order Sliding Modes and a High Gain Observer," *IREMOS International Review on Modelling & Simulations*, vol. 4, no. 3, pp. 1148-1155, Jun. 2011.
[17] B. Purwahyudi, *et al*., "RNN Based Rotor Flux and Speed Estimation of Induction Motor," *International Journal of Power Electronics and Drive System (IJPEDS)*, vol. 1, no. 1, pp. 58-64, 2011.
[18] Beltran B., Ahmed-Ali T., Benbouzid M.E.H., "Sliding mode power control of variable-speed wind energy conversion systems," *IEEE Trans. Energy Convers*., vol. 23, no. 2, pp. 551–558, 2008.
[19] Martinez, M.I., Susperregui, A., Tapia, G., *et al*., "Sliding-mode control of awind turbine-driven double-fed induction generator under non-ideal grid voltages," *IET Renew. Power Gener.*, vol. 7, no. 4, pp. 370–379, 2013.
[20] M. Abdur Razzak, Wahida Taskin Bhuiyan, Nawrin Islam Natasha, A.K.M. Muzahidul Islam, Muhamad Kamal Mohammed Amin, "Design of a Grid-connected Photovoltaic Inverter with Maximum Power Point Tracking using Perturb and Observe Technique," *International Journal of Power Electronics and Drive System (IJPEDS)*, vol. 7, no. 4, pp. 1212-1220, Dec 2016.
[21] Ramin Shirmohammadi, Vahid Rezanejad, and Aliajami, "The Compression of MPPT Methods in Small Sized Wind Power Plants," *Journal of Artificial Intelligence in Electrical Engineering*, vol. 3, no. 11, pp. 19-38, 2014.
[22] G. Rigatos, "A derivative-free Kalman Filtering approach for sensorless control of nonlinear systems," *IEEE International Symposium on Industrial Electronics*, pp. 2049 - 2054, 2010.
[23] N. Amuthan, *et al*., "Voltage sag ride through using Improved Adaptive Internal Model Controller for doubly fed induction generator wind farms," *Computers and Electrical Engineering*, 2013.
[24] I. Boldea, *et al*., *The induction machine handbook*, CRC Press; 2002.
[25] Moutchou *et al*., "MRAS-based sensorless speed backstepping control for induction machine, using a flux sliding mode observer," *Turkish Journal of Electrical Engineering & Computer Sciences*, vol. 23, pp. 187-200, 2015.

APPENDIX

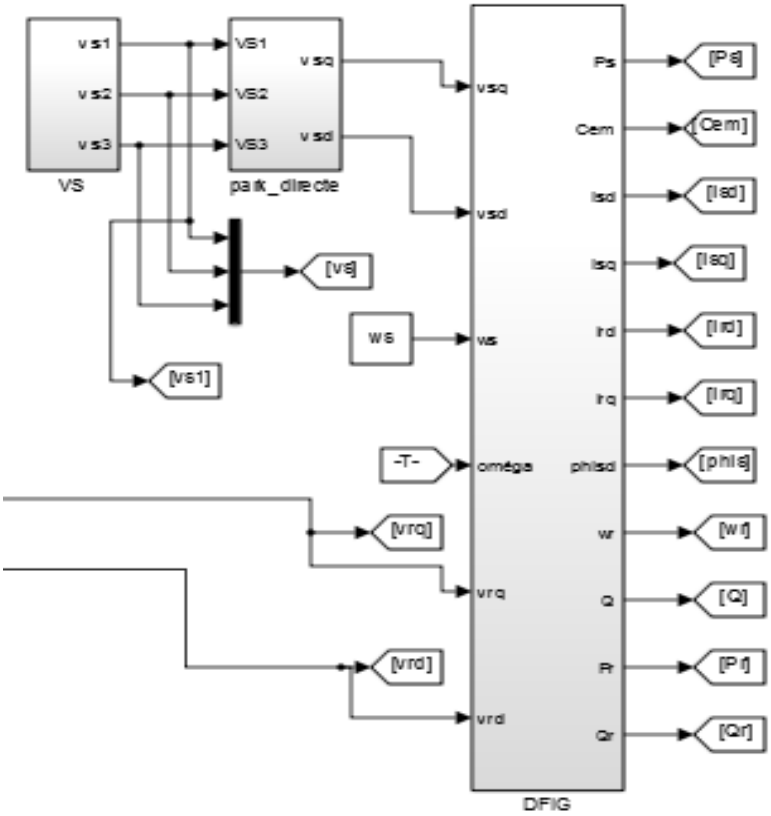

Figure 9. DFIG model

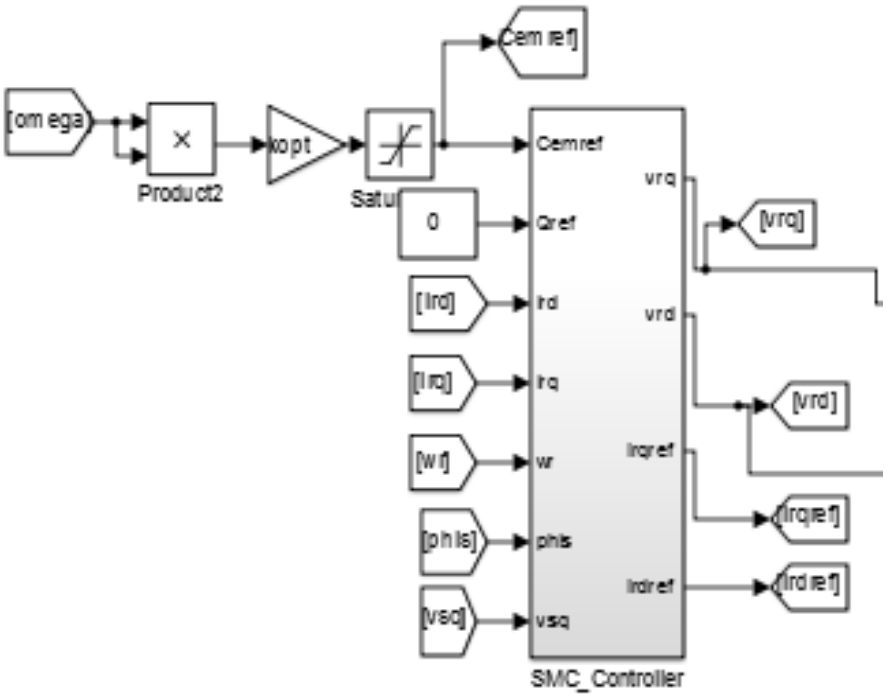

Figure 10. Second ordre sliding mode model